ZMIZ1 Variants Cause a Syndromic Neurodevelopmental Disorder

Raphael Carapito, Ekaterina L. Ivanova, Aurore Morlon, Linyan Meng, Anne Molitor, Eva Erdmann, Bruno Kieffer, Angélique Pichot, Lydie Naegely, Aline Kolmer, et al.

ZMIZ1 Variants Cause a Syndromic Neurodevelopmental Disorder

Raphael Carapito[1,2]*, Ekaterina L. Ivanova[3], Aurore Morlon[4], Linyan Meng[5,6], Anne Molitor[1], Eva Erdmann[3], Bruno Kieffer[3], Angélique Pichot[1], Lydie Naegely[1], Aline Kolmer[1], Nicodème Paul[1], Antoine Hanauer[1], Frédéric Tran Mau-Them[7], Nolwenn Jean-Marçais[7], Susan M. Hiatt[8], Gregory M. Cooper[8], Tatiana Tvrdik[9], Alison M. Muir[10], Clémantine Dimartino[11,12], Maya Chopra[13,14], Jeanne Amiel[11,12,13], Christopher T. Gordon[11,12], Fabien Dutreux[1], Aurore Garde[7], Christel Thauvin-Robinet[7], Xia Wang[5,6], Magalie S. Leduc[5,6], Meredith Phillips[15], Heather P. Crawford[15], Mary K. Kukolich[15], David Hunt[16], Victoria Harrison[16], Mira Kharbanda[16], Deciphering Developmental Disorders Study[17], University of Washington Center for Mendelian Genomics, Robert Smigiel[18], Nina Gold[19], Christina Y. Hung[19], David H. Viskochil[20], Sarah L. Dugan[20], Pinar Bayrak-Toydemir[20,9], Géraldine Joly-Helas[21], Anne-Marie Guerrot[21], Caroline Schluth-Bolard[22], Marlène Rio[12,13], Ingrid M. Wentzensen[23], Kirsty McWalter[23], Rhonda E. Schnur[23], Andrea M. Lewis[5,24], Seema R. Lalani[5,24], Noël Mensah-Bonsu[24], Jocelyn Ceraline[3,25], Zijie Sun[26], Rafal Ploski[27], Carlos A. Bacino[5,24], Heather C. Mefford[10], Laurence Faivre[7], Olaf Bodamer[19,28], Jamel Chelly[3,29], Bertrand Isidor[30], Seiamak Bahram[1,2]*

1 Laboratoire d'ImmunoRhumatologie Moléculaire, plateforme GENOMAX, INSERM UMR_S 1109, Faculté de Médecine, Fédération Hospitalo-Universitaire OMICARE, Fédération de Médecine Translationnelle de Strasbourg (FMTS), LabEx TRANSPLANTEX, Université de Strasbourg, 4 rue Kirschleger, 67085 Strasbourg, France.

2 Service d'Immunologie Biologique, Plateau Technique de Biologie, Pôle de Biologie, Nouvel Hôpital Civil, 1 place de l'Hôpital, 67091 Strasbourg, France

3 Institut de Génétique et de Biologie Moléculaire et Cellulaire, CNRS UMR 7104, INSERM U1258, Université de Strasbourg, 1 rue Laurent Fries, 67404 Illkirch, France.

4 BIOMICA SAS, 4 rue Boussingault, 67000 Strasbourg, France.

5 Department of Molecular and Human Genetics, Baylor College of Medicine, Houston, TX 77030, USA.

6 Baylor Genetics, Houston, TX 77021, USA.

7 Fédération Hospitalo-Universitaire Médecine Translationnelle et Anomalies du Développement (TRANSLAD), CHU de Dijon Bourgogne, 21079 Dijon, France; Inserm UMR1231 GAD, Génétique des Anomalies du Développement, Université de Bourgogne, 21079 Dijon, France.

8 HudsonAlpha Institute for Biotechnology, Huntsville, AL 35806, USA.

9 ARUP Laboratories, Salt Lake City, UT 84108 USA.

10 Department of Pediatrics, University of Washington, Seattle WA 98195, USA.

11 Laboratory of Embryology and Genetics of Human Malformations, INSERM UMR 1163, *Imagine* Institute, 75015 Paris, France.

12 Paris Descartes-Sorbonne Paris Cité Université, *Imagine* Institute, 75015 Paris, France.

13 Département de Génétique, Hôpital Necker-Enfants Malades, Assistance Publique Hôpitaux de Paris (AP-HP), Paris, France.

14 Discipline of Genetic Medicine, University of Sydney, Sydney 2050, Australia.

15 Cook Children's Medical Center, Fort Worth, TX 76102, USA.

16 Wessex Clinical Genetics Service, Princess Anne Hospital, Southampton SO16 5YA, UK.

17 The Wellcome Sanger Institute, Hinxton CB10 1SA, UK.

18 Department of Pediatrics and Rare Disorders, Wroclaw Medical University, 50-368 Wroclaw, Poland.

19 Division of Genetics and Genomics, Boston Children's Hospital, Harvard Medical School, Boston MA, 02115, USA.

20 Department of Pediatrics, Division of Medical Genetics, University of Utah School of Medicine, Salt Lake City, UT 84108, USA.

21 Department of Genetics, Rouen University Hospital, Normandy Centre for Genomic and Personalized Medicine, 76821 Rouen, France.

22 Department of Genetics, Hospices Civils de Lyon, GENDEV Team, Neurosciences Research Center of Lyon, INSERM U1028, CNRS UMR5292, UCBL1, 69677 Bron, France.

23 GeneDx Inc., Gaithersburg, MD 20877, USA.

24 Texas Children's Hospital, Houston TX 77030, USA.

25 Service d'Onco-Hématologie, Hôpitaux Universitaires de Strasbourg, 67091 Strasbourg, France.

26 Comprehensive Cancer Center and Beckman Research Institute, City of Hope, Duarte, CA 91010, USA.

27 Department of Medical Genetics, Warsaw Medical University, 02-106 Warsaw, Poland.

28 Broad Institute of MIT and Harvard University, Cambridge, MA 02142 USA.

29 Laboratoire de Diagnostic Génétique, Hôpitaux Universitaire de Strasbourg, 67000 Strasbourg, France.

30 Service de Génétique Médicale, Hôpital Hôtel-Dieu, CHU de Nantes, 44093 Nantes, France.

*To whom correspondence should be addressed: Seiamak Bahram and/or Raphael Carapito, both at Centre de Recherche d'Immunologie et d'Hématologie, 4 rue Kirschleger, 67085 Strasbourg Cedex France; e-mails: siamak@unistra.fr and/or carapito@unistra.fr

Key Words: *ZMIZ1*, intellectual disability, neurodevelopmental disorder, neuronal positioning, transcriptional coactivation.

Abstract

ZMIZ1 is a coactivator of several transcription factors, including p53, the androgen receptor and NOTCH1. Here, we report 19 subjects with intellectual disability and developmental delay carrying variants in *ZMIZ1*. The associated features include growth failure, feeding difficulties, microcephaly, facial dysmorphism, and various other congenital malformations. Fourteen unrelated subjects carried *de novo* heterozygous single nucleotide variants (SNVs) or single-base insertions/deletions, three siblings harbored a heterozygous single-base insertion, and two subjects had a balanced translocation disrupting *ZMIZ1* or involving a regulatory region of *ZMIZ1*. In total, we identified 13 point mutations that affect key protein regions, including a SUMO acceptor site, a central disordered alanine-rich motif, a proline-rich domain and a transactivation domain. All identified variants were absent from all available exome/genome databases. *In vitro*, ZMIZ1 showed impaired coactivation of the androgen receptor. *In vivo*, overexpression of *ZMIZ1* mutant alleles in developing mouse brains using *in utero* electroporation resulted in abnormal pyramidal neuron morphology, polarization and positioning, underscoring the importance of *ZMIZ1* in neural development and supporting mutations in *ZMIZ1* as the cause of a rare neurodevelopmental syndrome.

Main text

Intellectual disability (ID) defines a diverse group of neurodevelopmental disorders that have a global prevalence of approximately 1% [1]. ID is highly heterogeneous and can be categorized into syndromic and nonsyndromic forms. More than 1,000 underlying genetic causes of ID have been identified to date [2-4]. Some of the genes previously associated with ID encode transcriptional regulators and are structured within a group of conditions called "transcriptomopathies" [5-7]. Subjects with these syndromes may share a number of clinical features in addition to ID and developmental delay (DD), including growth restriction and facial dysmorphisms.

ZMIZ1 (also known as *ZIMP10* or *RAI17*, [MIM 607159]) is a transcriptional coregulator of the Protein Inhibitor of Activated STAT (PIAS)-like family. PIAS-like proteins do not bind DNA directly but regulate other DNA-binding transcription factors, generally through sumoylation [8]. In addition, ZMIZ1 enhances the transcriptional activity of the tumor suppressor protein p53 [9] and the androgen receptor (AR) [10]. *ZMIZ1* is also involved in the transcriptional activation of a subset of NOTCH1 target genes, including *MYC* ([MIM 190080]). Through its direct interaction with NOTCH1, *ZMIZ1* plays a role in T lymphocyte development [11; 12]. As NOTCH1 is directly involved in the regulation of cell fate during both neuronal and glial cell developments [13-15], a role for *ZMIZ1* in neural development is equally plausible. Like other PIAS, ZMIZ1 is predicted to function as an E3 SUMO ligase. Sharma *et al.* [10] indeed demonstrated that ZMIZ1 co-localizes with AR and SUMO-1 in the nucleus and forms a protein complex at replication foci. They also showed that ZMIZ1 enhances sumoylation of AR and that the increase of AR activity by ZMIZ1 is dependent on the sumoylation of the receptor using AR mutated at sumoylation sites [10]. In 2015, Cordova-Fletes *et al.* reported a girl with ID and neuropsychiatric symptoms with a *de novo* balanced translocation, t(10;19)(q22.3;q13.33) that resulted in gene fusion between *ZMIZ1* (chr10) and *PRR12* (chr19, [MIM 616633]) thereby disrupting the zinc-finger motif of *ZMIZ1* (however this study was by nature unable to attribute the observed phenotype to either *ZMIZ1* or *PRR12*) [16]. More recently, Liu et *al.* showed that an enhancer of *ZMIZ1* harbors recurrent single

nucleotide variations (SNVs) in autism spectrum disorder [17]. Finally, animal models also suggest a role for ZMIZ1 in embryonic development, as mice homozygous for a null mutation in *ZMIZ1* display embryonic lethality during organogenesis, with yolk sac vascular remodeling failure and abnormal embryonic vascular development [18].

Here, we report 19 subjects (16 unrelated) with a syndromic form of ID/DD due to variants in *ZMIZ1*, which were identified by whole-exome or genome sequencing. The compilation of this series of subjects resulted from a transatlantic collaborative effort between University of Strasbourg (Strasbourg, France), Nantes University Hospital (Nantes, France), Dijon University Hospital (Dijon, France), Rouen University Hospital (Rouen, France), Necker Hospital/*Imagine* Institute (Paris, France), Lyon University Hospitals (Lyon, France), Baylor Genetics Laboratories (Houston, TX, USA), ARUP Laboratories (Salt Lake City, UT, USA), HudsonAlpha Institute for Biotechnology (Huntsville, AL, USA), Princess Anne Hospital (Southampton, UK), Medical University of Warsaw (Warsaw, Poland), Boston Children's Hospital (Boston, MA, USA), University of Washington (Seattle, WA, USA) and GeneDx (Gaithersburg, MD, USA). The study was also partly facilitated by the web-based tools GeneMatcher [19], MyGene2 [20], DECIPHER [21] and Matchmaker Exchange [22]. All subjects were clinically assessed by at least one experienced clinical geneticist from the participating centers. All sequencing (whole exome, genome and Sanger) was performed after written informed consent for either clinical sequencing and/or center-specific institutional review board approved research sequencing. Consent for published images (Figure 1) were obtained from all parents/legal guardians. All procedures were performed in accordance with the Helsinki Declaration. The main clinical features of the cohort are summarized in Table 1. More detailed clinical information for all subjects is provided in Table S1 and Supplemental Note: Case Reports.

All subjects from the series exhibited ID/DD (n=19). Growth failure and feeding difficulties were each reported in 10 and 9 subjects, respectively. Five subjects had microcephaly (subjects #3, #5, #9, #16 and #19 with SD -2.2, -3.0, -2.2, -2.0 and -2.0, respectively). All subjects had additional neurological features, including motor delay (n=12),

speech delay (n=15), abnormal behavior (n=13), seizures (n=3), hypotonia (n=10) and hearing loss (n=4). Thirteen subjects had other congenital malformations, including ventricular septal defects (n=2), abnormal mitral valve (n=1), patent ductus arteriosus (n=1), renal pelviectasis (n=1), cryptorchidism (n=2), vesicoureteral reflux (n=3) and atrophic kidney (n=1). Eleven subjects had additional ophthalmologic anomalies, i.e., decreased vision (n=1), ptosis (n=3), glaucoma (n=1), hypermetropia (n=2), astigmatism (n=1), myopia (n=1), Duane syndrome (n=1), nasolacrimal duct stenosis (n=1), coloboma of the retina (n=1) and amblyopia (n=1). Nine subjects had skeletal defects including joint hypermobility (n=8), pectus excavatum (n=1), scoliosis (n=3), spondylolisthesis (n=1), and finally, abnormalities of the feet (bilateral 2/3 toe syndactyly n=6; cone-shaped epiphyses n=2; bilateral clubfeet n=2; short toes n=1), hands (short fingers n=6; long fingers n=1, tapered fingers n=1; brachydactyly n=1), and palate (n=3). Craniofacial dysmorphisms were observed in 16 subjects (see Figure 1, as well as Table S1 and Supplemental Note: Case Reports for details).

All *ZMIZ1* variants and genomic alterations reported in this work are detailed in Table 2. Protocols for single- or trio-based whole-exome/genome sequencing and Sanger sequencing were previously described [4; 23-28] (see also Supplemental Methods). None of the variants identified here were present in gnomAD [29], the Exome Variant Server [30], and an internal database of 550 exomes. Aside from one family (subjects #13, #14 and #15) for whom parental samples were unavailable, all variants were shown to be *de novo* (Figure S1). The variants were all predicted to be disease-causing by various bioinformatics tools and to affect specific functional domains of the protein (Table 2; Figure 2A). Two additional subjects (#18 and #19) with balanced *de novo* translocations between chromosomes X and 10 (46,XX,t(X;10)(q27;q23)), and 10 and 12 (46,XX,t(10;12)(q22.2;q24.3)) respectively, were identified by blood karyotyping. The breakpoints on the X chromosome (Xq27.3, chrX:143274164_143274161, GRCh37) and on chromosome 10 (10q22.3, chr10:80552343_80552344, GRCh37) for the t(X;10)(q27;q23) translocation, and on chromosome 12 (12q24.32, chr12:128533508_128533517, GRCh37) and chromosome 10

(10q22.3, chr10:81010865_81010871, GRCh37) for t(10;12)(q22.2;q24.3) translocation were defined by whole-genome sequencing (Table 2). While the t(10;12)(q22.2;q24.3) translocation of subject #19 disrupts the *ZMIZ1* gene, no gene is disrupted by t(X;10)(q27;q23) translocation in subject #18. However, the breakpoint on chromosome 10 in this subject is located 276 kb upstream of the *ZMIZ1* gene, where it disrupts a distal enhancer (position chr10:80559750-80568675) known to harbor recurrent SNVs in autism spectrum disorder subjects and predicted to interact with the *ZMIZ1* promoter [17]. Moreover, as detailed below, the deleterious effect of the translocations on *ZMIZ1* expression was further confirmed by quantitative RT-PCR analysis of *ZMIZ1* transcripts.

The ZMIZ1 protein sequence contains both folded domains and low-complexity regions predicted to be intrinsically disordered (Figure 2A). The folded domains include a tetratricopeptide repeat at the N-terminus extremity (1-120), which is involved in the interaction with NOTCH1, and an MIZ/SP-RING finger (727-804) acting as an adapter for sumoylation [31]. Disordered regions include two large proline-rich domains and an alanine-rich motif (280-305). Of note, most variants were found in these low-complexity regions, with the exception of p.Lys91Arg, which colocalizes with a SUMO acceptor site (Figure 2A). ZMIZ1 is, indeed, known to enhance AR sumoylation by its E3 SUMO ligase activity, which is essential for its coregulatory function [10; 32]. The alanine-rich domain 280-305 contains five variants (p.Ala287Thr, p.Thr296Lys, p.Thr296Ile, p.Thr298Ile and p.Thr300Met present in six unrelated subjects). The sequence of this domain (*AAAAAAAAVAAAAATATATATATVAA*) is evolutionarily conserved and specific to the ZMIZ1 protein (Figure S2). The p.Thr296Lys, p.Thr296Ile, p.Thr298Ile and p.Thr300Met variants suggest that a strict alternation of alanine-threonine repeats is required for the physiological function of ZMIZ1. This motif is flanked by regular motifs of glycine and proline residues, suggesting a possible role in phase transition (Figure 2B). Phase transitions due to sequences of low complexity are an emerging mechanism of transcriptional regulation, and disease-related variants in such regions have been shown to disrupt transcription [33-36]. Disruption of the alanine-threonine repeat by variants may therefore have a direct impact on the coregulation of transcription mediated by

ZMIZ1. Another series of seven variants is predicted to shorten or remove the C-terminal transactivation domain of the protein: (1) the four frameshift variants p.Gln920Profs*34, p.Met946Cysfs*61, p.Phe1008Leufs*7 and p.Thr1038Asnfs*4 each lead to a premature stop codon, (2) p.Ser870Ser is silent at the protein level but is part of an exonic splicing enhancer site for SF2/ASF (C[C/T]CCCTA) and SRp40 (CGTC[C/T]CC), (3) the c.3097-2A>G splice-site variant leads to the loss of an acceptor site (AG>GG) in the last intron of the gene, resulting in two alternative transcripts (Figure S3), and finally, (4) the p.Thr463Hisfs*1 variant affects the proline-rich domain 334-555 and is predicted to be translated into a protein that is shortened by more than half of its length (464 amino acids instead of 1067 amino acids). It is highly probable that these variants result in truncated proteins with an absent or shortened transactivation domain and, thus, reduced cotranscriptional activity.

We further assessed the expression of *ZMIZ1* at the mRNA level in peripheral blood from five subjects with point mutations (#1, #5, #8, #9 and #11), in an EBV-transformed lymphoblastoid cell line of subjects #18 with the t(X;10)(q27;q23) translocation and in peripheral blood of subject #19 with the t(10;12)(q22.2;q24.3) translocation. The expression level of *ZMIZ1* in subjects with point mutations was found to be similar to that in healthy controls (Figure S4A). This observation was true for subjects with missense variants (subject #1, c.899C>T; subject #5, c.893C>T and subject #9, c.887C>A) as well as for those with suspected or confirmed splice-site variants (subject #8, c.2610C>T and subject #11, c.3097-2A>G). In subject #18, the mRNA level was decreased compared to that in controls, supporting the presence of a position effect (Figure S4B). At the protein level, transfection of HeLa cells with wild-type or mutant (p.Lys91Arg, p.Thr300Met or Thr1038fs) *ZMIZ1* plasmids indicated nuclear localization (Figure S5).

As ZMIZ1 is a well-known AR coactivator [10], we sought to analyze the effect of three representative *ZMIZ1* mutations on this process. We cotransfected the HEK293T cell line with expression vectors containing the following cDNA constructs: *ZMIZ1* (wild-type, c.272A>G, c.899C>T or c.3112dupA), AR, renilla luciferase and a consensus androgen response element (ARE)-driven luciferase reporter. Luciferase activity was determined with

and without induction by the AR ligand dihydrotestosterone (DHT) (Figure 3A). Compared to wild-type ZMIZ1 protein, all three mutant proteins showed decreased induction of luciferase activity after the addition of DHT (although not statistically significant for the p.Lys91Arg mutant). These results indicate that *ZMIZ1* variants impair the coactivation activity of the protein.

Next, we sought to investigate the effect of the three *ZMIZ1* variants on neuronal positioning *in vivo* [37]. We first validated that the wild type and mutant proteins were stable (not degraded) when overexpressed in neuronal cells using the neuro2A cell line (Figure S6). We then used *in utero* electroporation to induce the overexpression of human *ZMIZ1* variants under the control of a CAG promoter together with a pCAGGS-IRES-Tomato (RFP) reporter in progenitor cells in the ventricular zone. Mice cortices were electroporated at embryonic day 14 (E14.5), and the distribution of electroporated cells was analyzed at E18.5. The relative percentage of electroporated RFP-positive cells was calculated for four different regions of the cortical wall: the ventricular and subventricular zones (VZ/SVZ); the intermediate zone (IZ) and the upper and lower cortical plate (CP) (Figure 3B). In brain sections expressing the empty vector control, the majority of the electroporated neurons were positioned within the upper layers of the CP. Likewise, overexpression of human WT-*ZMIZ1* showed a normal pattern of distribution, similar to that in the control. In contrast, *in utero* electroporation of *ZMIZ1* pathogenic variants resulted in impaired neuronal positioning at this stage with an accumulation of electroporated cells in the VZ/SVZ and IZ and a corresponding depletion of these cells in the upper CP. The phenotype of two variants, p.Lys91Arg and p.Thr300Met, appeared more severe than that of Thr1038fs, with approximately 60% of the electroporated cells remaining in the IZ and VZ/SVZ. In the third variant Thr1038fs, approximately 40% of electroporated cells remained in these regions, and interestingly, 25% was found in the lower CP, suggesting possible differences in the severity of consequences from the variants. Rescue experiments consisting of co-electroporation of the WT *ZMIZ1* plasmid along with different mutants showed a partial rescue of the WT phenotype only in the case of the p.Thr300Met variant (Figure S7). Moreover, a closer look

at the arrested cells in the IZ revealed striking morphological features. The majority of cells in the IZ were round; however, the cells emitting processes appeared aberrantly long and abnormally oriented (Figure 3C). This phenotype is in contrast with the expected dynamics and morphological changes of migrating neurons. Indeed, in the IZ, migrating newborn neurons adopt a bipolar morphology and extend a leading process towards the CP [38]. The presence of rounded cells and of cells with long, randomly oriented processes suggests the disruption of proper polarization. Abnormal morphology and polarization could underlie the inability of the cells to migrate properly. Together, these data suggest an important role for *ZMIZ1* in early stages of the postmitotic positioning of pyramidal neurons in the developing cerebral cortex.

Taken together, our data indicate that *ZMIZ1* plays an important role during embryonic development. High expression levels of *ZMIZ1* in craniofacial tissue and brain [18; 39] are consistent with the clinical phenotype of ID/DD and the craniofacial dysmorphism observed in 16 of the subjects included in this study. Moreover, in the brain, ZMIZ1 has been shown to interact with chromatin remodeling complex (nBAF) and activator protein 1 (AP-1), which regulate the activity of genes essential for normal synapse and dendrite development [40; 41]. During mouse embryogenesis, the expression of *ZMIZ1* was shown to be very dynamic, with a remarkable expression pattern in the limb buds; *ZMIZ1* expression was restricted to the interdigital region at limb stage S8(embryonic day 12) [18], an observation that is in line with syndactyly, which was observed in 6 of our subjects (Figure 1, Table 1, S1 and Supplemental Note: Case Reports). Furthermore, we showed here that overexpression of ZMIZ1 mutants in mouse progenitor cells impaired neuronal migration. This result might be explained by an effect on the well-known partner of ZMIZ1, NOTCH1, which has been shown to regulate neurite outgrowth in neuroblastoma cells [13] and to promote the acquisition of the first specialized cell type (i.e., radial glia) in the mouse forebrain during embryogenesis [14].

In conclusion, we describe a neurodevelopmental disorder caused by *de novo* heterozygous point mutations or rearrangement of the *ZMIZ1* gene. Further studies are needed to definitively conclude as to a mechanism of action of these variants.

Acknowledgments

We thank Drs Olivier Pourquié and Clifford Tabin (Harvard Medical School) for discussions on limb development. We thank Dr. Kevin Bowling (HudsonAlpha Institute for Biotechnology) for computation of CADD scores. We are grateful to the families who participated in this study. This work was supported by grants from the Agence Nationale de la Recherche (ANR), the INSERM (UMR_S 1109) and the Institut Universitaire de France (IUF) to SB; the European regional development fund (European Union) INTERREG V program (project n°3.2 TRIDIAG) to RC and SB; MSD Avenir grant (Autogen project) to SB; the French Ministry of Health (DGOS) and the French National Agency for Research (ANR) (PRTS 2013) grants to CSB; the MSD Avenir (DevoDecode project) and ANR to JA, CTG and CD; and a grant from the National Human Genome Research Institute to GMC (UM1HG007301). The DDD study presents independent research commissioned by the Health Innovation Challenge Fund [grant number HICF-1009-003]; see *Nature* 25533962 or www.ddduk.org/access.html for full acknowledgement. This study used data shared through MyGene2.org. Funding for MyGene2 was provided by the National Institutes of Health/National Human Genome Research Institute and National Heart Lung and Blood Institute through the University of Washington Center for Mendelian Genomics (2UM1HG006493-05) and by Wellcome Trust, U.S. National Institutes of Health, and Howard Hughes Medical Institute through the Open Science Prize. HCM has grant funding from NIH (NINDS NS069605). Sequencing at University of Washington was provided by the University of Washington Center for Mendelian Genomics (UW-CMG) and was funded by NHGRI and NHLBI grants UM1 HG006493 and U24 HG008956. The content is therefore solely the responsibility of the authors and does not necessarily represent the official views of the National Institutes of Health.

Declaration of Interests

Ingrid M. Wentzensen, Kirsty McWalter, and Rhonda E. Schnur are employees of GeneDx, Inc., a wholly owned subsidiary of OPKO Health, Inc. The other authors declare no competing interests.

Supplemental Data

Supplemental Case Reports: Detailed clinical history of the reported subjects.

Supplemental Figures and Legends S1-S6.

supplemental Tables S1-S2.

Supplemental Methods: Supplemental materials and methods

Supplemental References

Web Resources

- gnomAD browser, http://gnomad.broadinstitute.org/
- GATK resources, https://www.broadinstitute.org/gatk/guide/article?id=1247
- GeneMatcher, https://genematcher.org/
- NHLBI Exome Sequencing Project (ESP) Exome Variant Server, http://evs.gs.washington.edu/EVS/
- OMIM, http://www.omim.org/
- PolyPhen-2 v.2.2.2, http://genetics.bwh.harvard.edu/pph2/
- RefSeq, http://www.ncbi.nlm.nih.gov/RefSeq
- SIFT v.1.03, http://sift.bii.a-star.edu.sg/
- Mutation Taster, http://www.mutationtaster.org/
- Matchmaker Exchange, https://www.matchmakerexchange.org/
- MyGene2, https://mygene2.org/MyGene2/
- ESEfinder, http://exon.cshl.edu/ESE/
- ExAC Browser, http://exac.broadinstitute.org/

- Decipher https://decipher.sanger.ac.uk/

Accession Numbers

The *ZMIZ1* variants reported in this paper have been submitted to [ClinVar]:[SUB4881332].

Tables

Table 1. Summary of the Major Phenotypic Features of Subjects with *ZMIZ1* Variants

Subjects	#1	#2	#3	#4	#5	#6	#7	#8	#9	#10	#11	#12	#13	#14[b]	#15[b]	#16	#17	#18	#19
Enrollment Center	Nantes/ France	Houston/ USA	Houston/ USA	Houston/ USA	Dijon/ France	Huntsville/ USA	Huntsville/ USA	Salt Lake City/USA	Salt Lake City/USA	Southampton/UK	Boston/ USA	Warsaw/ Poland	Houston/ USA	Houston/ USA	Houston/ USA	Paris/ France	Seattle/ USA	Rouen/ France	Paris/ France
***ZMIZ1* variant[a]**	c.899C>T (p.Thr300Met)	c.859G>A (p.Ala287Thr)	c.3112dupA (p.Thr1038Asnfs*4)	c.899C>T (p.Thr300Met)	c.893C>T (p.Thr298Ile)	c.2752dupC (p.Gln920Profs *34)	c.272A>G (p.Lys91Arg)	c.2610C>T (p.Ser870Ser)	c.887C>A (p.Thr296Lys)	c.1386dupC (p.Thr463Hisfs *14)	c.3097-2A>G (p.?)	c.3021delC (p.Phe1008Leufs*7)	c.1386dupC (p.Thr463Hisfs *14)	c.1386dupC (p.Thr463Hisfs *14)	c.1386dupC (p.Thr463Hisfs *14)	c.887C>T (p.Thr296Ile)	c.2835delT (p.Met946Cysfs*61)	t(X;10)(q27.3;q22.3)	t(10;12)(q22.2;q24.3)
Inheritance	*de novo*	*de novo*	*de novo*	*de novo*	*de novo*	*de novo*	*de novo*	*de novo*	*de novo*	*de novo*	*de novo*	*de novo*	unknown	unknown	unknown	*de novo*	*de novo*	*de novo*	*de novo*
Gender	male	female	female	female	male	female	female	male	female	female	male	male	female	male	male	female	female	female	female
Age at last visit	11 y, 8 m	12 y, 3 m	12 y, 3 m	1 y, 6 m	5 y, 9 m	20 y	3 y	6 y, 7 m	8 y, 6 m	19 y	1 y, 4 m	3 y, 6 m	7 y	10 y	11 y	7 y	12 y, 17 m	17 y	2y,9 m
Weight (g) birth (SD)	3,520(+0.4)	ND	ND	ND	2,185 (-2.8)	3,090 (-0.2)	ND	ND	2,135 (-2.7)	2,380 (-2)	2,780 (-1.4)	3,300 (0)	ND	ND	3,165 (-0.4)	2200 (-2.5)	2899 (-0.4)	2,510 (-1.8)	2,560 (-1.8)
Length (cm) birth (SD)	51 (+0.5)	ND	ND	ND	44 (-3)	ND	ND	ND	47 (-1.1)	ND	47 (-1.5)	55 (+2.6)	ND	ND	ND	45 (-2.2)	45 (-2.2)	47 (-1.1)	47.5 (-1.1)
OFC (cm) birth (SD)	35 (+0.4)	ND	ND	ND	30 (-3.5)	ND	ND	ND	30.5 (-2.9)	ND	33.5 (-1.3)	34 (-0.4)	ND	ND	ND	32.5 (-1.2)	33 (-1.2)	32.5 (-1.2)	32 (-1.2)
Growth																			
Growth failure yes/no	no	yes (weight)	no	ND	yes	yes (weight)	NA	no	yes	yes	no	no	yes	yes	yes	yes	yes	no	no
Weight (kg) last visit (SD)	48.7 (+2.0)	32.7 (-1.5)	56.7 (+1.2)	ND	15.3 (-2.4)	56.7 (-0.2)	12.25 (-1.0)	25.9 (+1.0)	20.0 (-2.1)	41.45 (-2.6)	11 (-0.9)	17 (+0.9)	22.5 (-0.1)	27.4 (-0.9)	45.9 (+1.1)	20 (-0.5)	63.1 (+1.4)	83.3 (>+4)	11.5 (-1)
Height (cm) last visit (SD)	148.5 (-1.0)	150.7 (-0.3)	152.25 (-0.1)	ND	99 (-3.0)	139.7 (-3.6)	86.37 (-2.1)	116.7 (-0.5)	121.5 (-1.6)	137.6 (-4.3)	81 (-1.0)	106 (+1.7)	115 (-1.3)	126.8 (-1.8)	121.6 (-3.4)	114 (-1.0)	158.1 (+0.3)	157 (-0.5)	89 (-0.6)
OFC (cm) last visit (SD)	53 (-1.0)	55.7 (+1.4)	50.25 (-2.2)	ND	47.7 (-3.0)	54 (-0.3)	NA	52 (0.0)	49.0 (-2.2)	53 (-1.8)	46 (-1.6)	51 (+0.1)	49.4 (-1.5)	50.3 (-1.8)	52.1 (-0.9)	48.5 (-2.0)	53.7 (0.0)	56 (+1)	46 (-2)
Feeding difficulties	-	-	ND	+	+	+	+	ND	+	+	+	+	-	-	-	+	-	-	-
Neurological Abnormalities																			
Intellectual disability	+	+	+	+	+	+	+	+	+	+	+	+	+	+	+	+	+	+	+
Motor delay	+	-	-	+	+	-	+	+	+	+	+	+	ND	ND	ND	+	-	+	+
Speech delay	+	-	-	ND	+	+	+	+	+	+	+	+	+	+	ND	+	+	+	+
Abnormal behavior	-	+	+	ND	+	+	ND	+	+	+	+	+	-	+	ND	+	+	+	-
Seizures	-	-	ND	+	-	-	-	+	-	-	-	-	-	-	-	-	+	-	-
Hypotonia	+	-	-	ND	+	-	ND	ND	-	-	+	+	+	-	+	+	+	+	+
Hearing loss	-	-	+	-	+	-	-	-	-	-	-	-	+	-	-	+	-	-	-
Brain Abnormalities MRI	+	-	-	-	ND	+	-	-	ND	+	ND	ND	+	ND	+	+	+	-	-
Congenital Malformations																			
Cardiac	-	+	-	ND	+	-	ND	+	-	-	-	-	-	-	-	-	+	-	-

Urogenital/kidney	-	+	-	+	ND	+	ND	ND	+	-	+	+	-	-	+	-	-	+	-
Eye	-	+	+	+	+	+	ND	ND	+	+	+	-	+	+	-	-	+	-	-
Craniofacial dysmorphism	+	+	+	+	+	-	ND	+	+	+	+	+	+	+	+	+	+	+	-
Others	-	-	-	-	-	-	-	-	-	+	+	+	-	-	-	-	+	+	-
Skeletal Abnormalities																			
Joint hypermobility	-	+	-	+	-	-	ND	+	-	+	-	-	+	-	+	+	-	+	-
Pectus deformity	-	+	-	ND	-	-	ND	-	-	-	-	-	-	-	-	-	-	-	-
Thorax	+	+	-	ND	-	-	ND	-	+	-	-	-	-	-	-	-	+	-	-
Hands	+	+	-	ND	-	-	ND	+	+	+	-	+	-	-	+	+	-	+	-
Feet	+	+	+	+	+	-	ND	+	+	+	-	-	-	-	-	+	+	+	-
Palate	-	-	ND	+	ND	-	ND	ND	+	-	+	-	-	-	-	+	-	-	-

[a] Positions refer to GenBank transcript NM_020338.3. Nucleotide numbering uses +1 as the A of the ATG translation initiation codon in the reference sequence, with the initiation codon as codon 1.
[b] Subjects #14 and #15 are siblings of subject #13.
Abbreviations are as follows: y, years; m, months; ND, not determined; SD, standard deviation; OFC, occipitofrontal circumference; and MRI, magnetic resonance imaging.
More comprehensive information regarding clinical features could be found in Table S1 and Supplemental Note: Case Reports.

Table 2. Sequence Changes Identified

Subject No.	Nucleotide alteration [a]	Coding sequence alteration [b]	Amino acid alteration	SIFT [c]	LRT [d]	GERP++ [e]	PhyloP [f]	Polyphen [g]	CADD [h]	MutationTaster
1,4	chr10:81052055C>T	c.899C>T	p.Thr300Met	0	0.001	5.16	5.494	1	26.8	disease-causing
2	chr10:81052015G>A	c.859G>A	p.Ala287Thr	0	0.001	5.16	5.406	0.998	27.3	disease-causing
3	chr10:81072414_81072415insA	c.3112dupA	p.Thr1038Asnfs*4	NA	NA	5.16	5.572	NA	35	disease-causing
5	chr10:81052049C>T	c.893C>T	p.Thr298Ile	0.001	0.001	5.16	5.494	1	25.8	disease-causing
6	chr10:81067244_81067245insC	c.2752dupC	p.Gln920Profs*34	NA	NA	4.57	5.306	NA	35	disease-causing
7	chr10:80976023A>G	c.272A>G	p.Lys91Arg	0.032	0.004	5.3	4.442	0.956	27.1	disease-causing
8	chr10:81066043C>T	c.2610C>T [i]	p.Ser870Ser	NA	NA	0.619	-0.048	NA	6.092	disease-causing
9	chr10:81052043C>A	c.887C>A	p.Thr296Lys	0.001	0.001	5.16	5.494	1	25.6	disease-causing
10,13,14,15	chr10:81056383_81056384insC	c.1386dupC	p.Thr463Hisfs*14	NA	NA	4.96	2.061	NA	33	disease-causing
11	chr10:81072397A>G	c.3097-2A>G [j]	?	NA	NA	5.16	4.614	NA	34	disease-causing
12	chr10:81070866_81070866delC	c.3021delC	p.Phe1008Leufs*7	NA	NA	4.72	4.438	NA	35	disease-causing
16	chr10:81052043C>T	c.887C>T	p.Thr296Ile	0.11	0.001	5.16	5.497	1	25.4	disease-causing
17	chr10:81067328_81067329delTG	c.2835delT	p.Met946Cysfs*61	NA	NA	NA	NA	NA	35	disease-causing
18	t(X;10)(q27.3;q22.3)	NA	NA	NA	NA	NA	NA	NA	NA	NA
19	t(10;12)(q22.2;q24.3)	NA	NA	NA	NA	NA	NA	NA	NA	NA

Predictive analyses were performed with MutationTaster [42], Polyphen-2 v2.2.2r398 [43], GATK analysis toolkit [44] and ESEfinder [45]. All variants were absent from the Exome Variant Server and the gnomAD database.
NA, not applicable

[a] Positions refer to Hg19 (GRCh37).

[b] Positions refer to GenBank transcript NM_020338.

[c] Function prediction tool based on protein sequence conservation among homologs. Variants with scores between 0 and 0.05 are considered deleterious.

[d] DNA sequence evolutionary model expressed as a p-value.

[e] GERP++NR score: DNA conservation score.

[f] Vertebrate PhyloP scores. Values vary between -20 and +9.873. Sites predicted to be conserved are assigned positive scores, while sites predicted to be fast-evolving are assigned negative scores.

[g] Polyphen2_HDIV_score: variants with scores between 0.85 and 1.0 are predicted to be damaging with high confidence.

[h] CADDv1.4 scores ranges from 1 to 99, with a higher score indicating greater deleteriousness.

[i] Probable impact on splicing: part of CTCCCTA (ESE SF2/ASF) and CGTCTCC (ESE SRp40)

[j] Acceptor splice site lost

Figure Legends

Figure 1. Topographical Images of Subjects with *ZMIZ1* Variants

Figure 2. Domain Organization of ZMIZ1 and Its Variants from Affected Subjects

(A) Schematic representation of ZMIZ1 and 10 variants identified in 12 families. See Table 2 for DNA sequence changes in the subjects. The splice variant c.3097-2A>G and the t(10;19)(q22.3;q13.33) translocation are not represented here. TPR: tetratricopeptide repeat; SUMO: SUMO acceptor site; NLS: nuclear localization signal; MIZ: SP-RING/MIZ domain, TAD: transactivation domain. **(B)** Hydrophobic cluster analysis (HCA) of the alanine-rich region with predictions of intrinsically disordered regions from IUPRED [46] performed with the Medor Metaserver [47]. Symbols are used to represent amino acids with peculiar structural properties (star for proline, black diamond for glycine, square for threonine, and dotted square for serine, which may be either exposed or buried). Phase transition or phase separation has been put forward as a general mechanism for the transient formation of cellular bodies that behaves as liquid droplet. The occurrence of stochastic liquid-liquid phase transitions within a cell nucleus provides an interesting framework to explain recent experimental observations on the transcriptional regulation in higher eukaryotes [48].

Figure 3. *In Vitro* and *In Vivo* Effects of *ZMIZ1* Variants

(A) Effect of *ZMIZ1* variants on DHT-induced AR activity, as determined by the ARE-luciferase assay. HEK 293T cells were cultivated with 1 nM DHT or without DHT (ethanol as vehicle) and transiently transfected with 30 ng of *ZMIZ1* expression constructs in combination with 5 ng of pEGFP-ARwt (wild-type AR expression plasmid), 150 ng of pARE-luc (androgen response element (ARE)-driven luciferase reporter plasmid) and 20 ng of pRenilla-luc (renilla luciferase expression vector for normalization). The total amount of plasmids per well was kept constant by adding empty vectors as needed. Control

transfections without the pEGFP-ARwt or the ZMIZ1 vectors were also performed. Transfection experiments were repeated three times in quadruplicate. Relative luciferase units (RLUs) are presented as the mean ± SEM. Two-tailed t-test, * $p < 0.05$, ** $p < 0.01$, *** $p<0.001$. **(B)** Effect of *ZMIZ1* variants on neuronal migration and positioning. cDNA constructions were coelectroporated with an RFP-encoding reporter construction (dt-Tomato) in progenitor cells adjacent to the ventricle of E14.5 embryonic mouse cortices. Analyses were performed at E18.5. Images show coronal sections of E18.5 brains electroporated at E14.5 with either a control vector, WT *ZMIZ1* or one of the three mutated forms of *ZMIZ1*. Sections were stained with 4′,6-diamidino-2-phenylindole (DAPI). CP, cortical plate; IZ, intermediate zone; and VZ/SVZ, ventricular zone/subventricular zone. Scale bar, 50 μm. Histograms present the quantification of the percentage of fluorescent neurons in 4 different regions: upper and lower CP, IZ, and VZ/SVZ. Data are presented as the mean ± SEM, Two-way ANOVA with Tukey's multiple comparisons test, * $p < 0.05$, ** $p < 0.01$, *** $p < 0.001$, and **** $p < 0.0001$ compared to an empty vector control. **(C)** Morphological features of cells accumulated in the IZ with the three ZMIZ1 variants. Arrow shows cells with long and abnormally oriented processes. Double arrow shows a bipolar cell with a leading process oriented towards the VZ. Scale bar, 50 μm.

References

1. Maulik, P.K., Mascarenhas, M.N., Mathers, C.D., Dua, T., and Saxena, S. (2011). Prevalence of intellectual disability: a meta-analysis of population-based studies. Research in developmental disabilities 32, 419-436.

2. Gilissen, C., Hehir-Kwa, J.Y., Thung, D.T., van de Vorst, M., van Bon, B.W., Willemsen, M.H., Kwint, M., Janssen, I.M., Hoischen, A., Schenck, A., et al. (2014). Genome sequencing identifies major causes of severe intellectual disability. Nature 511, 344-347.

3. (2015). Large-scale discovery of novel genetic causes of developmental disorders. Nature 519, 223-228.

4. Wright, C.F., Fitzgerald, T.W., Jones, W.D., Clayton, S., McRae, J.F., van Kogelenberg, M., King, D.A., Ambridge, K., Barrett, D.M., Bayzetinova, T., et al. (2015). Genetic

diagnosis of developmental disorders in the DDD study: a scalable analysis of genome-wide research data. Lancet 385, 1305-1314.

5. Izumi, K. (2016). Disorders of Transcriptional Regulation: An Emerging Category of Multiple Malformation Syndromes. Molecular syndromology 7, 262-273.

6. Parenti, I., Teresa-Rodrigo, M.E., Pozojevic, J., Ruiz Gil, S., Bader, I., Braunholz, D., Bramswig, N.C., Gervasini, C., Larizza, L., Pfeiffer, L., et al. (2017). Mutations in chromatin regulators functionally link Cornelia de Lange syndrome and clinically overlapping phenotypes. Human genetics 136, 307-320.

7. Yuan, B., Pehlivan, D., Karaca, E., Patel, N., Charng, W.L., Gambin, T., Gonzaga-Jauregui, C., Sutton, V.R., Yesil, G., Bozdogan, S.T., et al. (2015). Global transcriptional disturbances underlie Cornelia de Lange syndrome and related phenotypes. The Journal of clinical investigation 125, 636-651.

8. Shuai, K., and Liu, B. (2005). Regulation of gene-activation pathways by PIAS proteins in the immune system. Nature reviews Immunology 5, 593-605.

9. Lee, J., Beliakoff, J., and Sun, Z. (2007). The novel PIAS-like protein hZimp10 is a transcriptional co-activator of the p53 tumor suppressor. Nucleic acids research 35, 4523-4534.

10. Sharma, M., Li, X., Wang, Y., Zarnegar, M., Huang, C.Y., Palvimo, J.J., Lim, B., and Sun, Z. (2003). hZimp10 is an androgen receptor co-activator and forms a complex with SUMO-1 at replication foci. The EMBO journal 22, 6101-6114.

11. Pinnell, N., Yan, R., Cho, H.J., Keeley, T., Murai, M.J., Liu, Y., Alarcon, A.S., Qin, J., Wang, Q., Kuick, R., et al. (2015). The PIAS-like Coactivator Zmiz1 Is a Direct and Selective Cofactor of Notch1 in T Cell Development and Leukemia. Immunity 43, 870-883.

12. Rakowski, L.A., Garagiola, D.D., Li, C.M., Decker, M., Caruso, S., Jones, M., Kuick, R., Cierpicki, T., Maillard, I., and Chiang, M.Y. (2013). Convergence of the ZMIZ1 and NOTCH1 pathways at C-MYC in acute T lymphoblastic leukemias. Cancer research 73, 930-941.

13. Franklin, J.L., Berechid, B.E., Cutting, F.B., Presente, A., Chambers, C.B., Foltz, D.R., Ferreira, A., and Nye, J.S. (1999). Autonomous and non-autonomous regulation of mammalian neurite development by Notch1 and Delta1. Current biology : CB 9, 1448-1457.

14. Gaiano, N., Nye, J.S., and Fishell, G. (2000). Radial glial identity is promoted by Notch1 signaling in the murine forebrain. Neuron 26, 395-404.

15. Angulo-Rojo, C., Manning-Cela, R., Aguirre, A., Ortega, A., and Lopez-Bayghen, E. (2013). Involvement of the Notch pathway in terminal astrocytic differentiation: role of PKA. ASN neuro 5, e00130.

16. Cordova-Fletes, C., Dominguez, M.G., Delint-Ramirez, I., Martinez-Rodriguez, H.G., Rivas-Estilla, A.M., Barros-Nunez, P., Ortiz-Lopez, R., and Neira, V.A. (2015). A de novo t(10;19)(q22.3;q13.33) leads to ZMIZ1/PRR12 reciprocal fusion transcripts in a girl with intellectual disability and neuropsychiatric alterations. Neurogenetics 16, 287-298.

17. Liu, Y., Liang, Y., Cicek, A.E., Li, Z., Li, J., Muhle, R.A., Krenzer, M., Mei, Y., Wang, Y., Knoblauch, N., et al. (2018). A Statistical Framework for Mapping Risk Genes from De Novo Mutations in Whole-Genome-Sequencing Studies. American journal of human genetics 102, 1031-1047.

18. Rodriguez-Magadan, H., Merino, E., Schnabel, D., Ramirez, L., and Lomeli, H. (2008). Spatial and temporal expression of Zimp7 and Zimp10 PIAS-like proteins in the developing mouse embryo. Gene expression patterns : GEP 8, 206-213.

19. Sobreira, N., Schiettecatte, F., Valle, D., and Hamosh, A. (2015). GeneMatcher: a matching tool for connecting investigators with an interest in the same gene. Human mutation 36, 928-930.

20. MyGene2. NHGRI/NHLBI University of Washington-Center for Mendelian Genomics (UW-CMG), Seattle, WA (URL: http://www.mygene2.org accessed 06/02/2018).

21. Firth, H.V., Richards, S.M., Bevan, A.P., Clayton, S., Corpas, M., Rajan, D., Van Vooren, S., Moreau, Y., Pettett, R.M., and Carter, N.P. (2009). DECIPHER: Database of Chromosomal Imbalance and Phenotype in Humans Using Ensembl Resources. American journal of human genetics 84, 524-533.

22. Philippakis, A.A., Azzariti, D.R., Beltran, S., Brookes, A.J., Brownstein, C.A., Brudno, M., Brunner, H.G., Buske, O.J., Carey, K., Doll, C., et al. (2015). The Matchmaker Exchange: a platform for rare disease gene discovery. Human mutation 36, 915-921.

23. Bowling, K.M., Thompson, M.L., Amaral, M.D., Finnila, C.R., Hiatt, S.M., Engel, K.L., Cochran, J.N., Brothers, K.B., East, K.M., Gray, D.E., et al. (2017). Genomic diagnosis for children with intellectual disability and/or developmental delay. Genome medicine 9, 43.

24. Carapito, R., Konantz, M., Paillard, C., Miao, Z., Pichot, A., Leduc, M.S., Yang, Y., Bergstrom, K.L., Mahoney, D.H., Shardy, D.L., et al. (2017). Mutations in signal recognition particle SRP54 cause syndromic neutropenia with Shwachman-Diamond-like features. The Journal of clinical investigation 127, 4090-4103.

25. Nambot, S., Thevenon, J., Kuentz, P., Duffourd, Y., Tisserant, E., Bruel, A.L., Mosca-Boidron, A.L., Masurel-Paulet, A., Lehalle, D., Jean-Marcais, N., et al. (2018). Clinical whole-exome sequencing for the diagnosis of rare disorders with congenital anomalies and/or intellectual disability: substantial interest of prospective annual reanalysis. Genetics in medicine : official journal of the American College of Medical Genetics 20, 645-654.

26. Ploski, R., Pollak, A., Muller, S., Franaszczyk, M., Michalak, E., Kosinska, J., Stawinski, P., Spiewak, M., Seggewiss, H., and Bilinska, Z.T. (2014). Does p.Q247X in TRIM63 cause human hypertrophic cardiomyopathy? Circulation research 114, e2-5.

27. Tanaka, A.J., Cho, M.T., Millan, F., Juusola, J., Retterer, K., Joshi, C., Niyazov, D., Garnica, A., Gratz, E., Deardorff, M., et al. (2015). Mutations in SPATA5 Are Associated with Microcephaly, Intellectual Disability, Seizures, and Hearing Loss. American journal of human genetics 97, 457-464.

28. Yang, Y., Muzny, D.M., Reid, J.G., Bainbridge, M.N., Willis, A., Ward, P.A., Braxton, A., Beuten, J., Xia, F., Niu, Z., et al. (2013). Clinical whole-exome sequencing for the

diagnosis of mendelian disorders. The New England journal of medicine 369, 1502-1511.

29. Lek, M., Karczewski, K.J., Minikel, E.V., Samocha, K.E., Banks, E., Fennell, T., O'Donnell-Luria, A.H., Ware, J.S., Hill, A.J., Cummings, B.B., et al. (2016). Analysis of protein-coding genetic variation in 60,706 humans. Nature 536, 285-291.

30. Exome Variant Server, N.G.E.S.P.E., Seattle, WA (URL: http://evs.gs.washington.edu/EVS/) [accessed in august 2018].

31. Yunus, A.A., and Lima, C.D. (2009). Structure of the Siz/PIAS SUMO E3 ligase Siz1 and determinants required for SUMO modification of PCNA. Molecular cell 35, 669-682.

32. Beliakoff, J., and Sun, Z. (2006). Zimp7 and Zimp10, two novel PIAS-like proteins, function as androgen receptor coregulators. Nuclear receptor signaling 4, e017.

33. Friedman, M.J., Shah, A.G., Fang, Z.H., Ward, E.G., Warren, S.T., Li, S., and Li, X.J. (2007). Polyglutamine domain modulates the TBP-TFIIB interaction: implications for its normal function and neurodegeneration. Nature neuroscience 10, 1519-1528.

34. Kovar, H. (2011). Dr. Jekyll and Mr. Hyde: The Two Faces of the FUS/EWS/TAF15 Protein Family. Sarcoma 2011, 837474.

35. Patel, A., Lee, H.O., Jawerth, L., Maharana, S., Jahnel, M., Hein, M.Y., Stoynov, S., Mahamid, J., Saha, S., Franzmann, T.M., et al. (2015). A Liquid-to-Solid Phase Transition of the ALS Protein FUS Accelerated by Disease Mutation. Cell 162, 1066-1077.

36. Chong, S., Dugast-Darzacq, C., Liu, Z., Dong, P., Dailey, G.M., Cattoglio, C., Heckert, A., Banala, S., Lavis, L., Darzacq, X., et al. (2018). Imaging dynamic and selective low-complexity domain interactions that control gene transcription. Science.

37. Saillour, Y., Broix, L., Bruel-Jungerman, E., Lebrun, N., Muraca, G., Rucci, J., Poirier, K., Belvindrah, R., Francis, F., and Chelly, J. (2014). Beta tubulin isoforms are not interchangeable for rescuing impaired radial migration due to Tubb3 knockdown. Human molecular genetics 23, 1516-1526.

38. Noctor, S.C., Martinez-Cerdeno, V., Ivic, L., and Kriegstein, A.R. (2004). Cortical neurons arise in symmetric and asymmetric division zones and migrate through specific phases. Nature neuroscience 7, 136-144.

39. Beliakoff, J., Lee, J., Ueno, H., Aiyer, A., Weissman, I.L., Barsh, G.S., Cardiff, R.D., and Sun, Z. (2008). The PIAS-like protein Zimp10 is essential for embryonic viability and proper vascular development. Molecular and cellular biology 28, 282-292.

40. Wu, J.I., Lessard, J., Olave, I.A., Qiu, Z., Ghosh, A., Graef, I.A., and Crabtree, G.R. (2007). Regulation of dendritic development by neuron-specific chromatin remodeling complexes. Neuron 56, 94-108.

41. Li, X., Zhu, C., Tu, W.H., Yang, N., Qin, H., and Sun, Z. (2011). ZMIZ1 preferably enhances the transcriptional activity of androgen receptor with short polyglutamine tract. PloS one 6, e25040.

42. Schwarz, J.M., Cooper, D.N., Schuelke, M., and Seelow, D. (2014). MutationTaster2: mutation prediction for the deep-sequencing age. Nature methods 11, 361-362.

43. Adzhubei, I.A., Schmidt, S., Peshkin, L., Ramensky, V.E., Gerasimova, A., Bork, P., Kondrashov, A.S., and Sunyaev, S.R. (2010). A method and server for predicting damaging missense mutations. Nature methods 7, 248-249.

44. McKenna, A., Hanna, M., Banks, E., Sivachenko, A., Cibulskis, K., Kernytsky, A., Garimella, K., Altshuler, D., Gabriel, S., Daly, M., et al. (2010). The Genome Analysis Toolkit: a MapReduce framework for analyzing next-generation DNA sequencing data. Genome research 20, 1297-1303.

45. Cartegni, L., Wang, J., Zhu, Z., Zhang, M.Q., and Krainer, A.R. (2003). ESEfinder: A web resource to identify exonic splicing enhancers. Nucleic acids research 31, 3568-3571.

46. Dosztanyi, Z., Csizmok, V., Tompa, P., and Simon, I. (2005). IUPred: web server for the prediction of intrinsically unstructured regions of proteins based on estimated energy content. Bioinformatics 21, 3433-3434.

47. Lieutaud, P., Canard, B., and Longhi, S. (2008). MeDor: a metaserver for predicting protein disorder. BMC genomics 9 Suppl 2, S25.

48. Hnisz, D., Shrinivas, K., Young, R.A., Chakraborty, A.K., and Sharp, P.A. (2017). A Phase Separation Model for Transcriptional Control. Cell 169, 13-23.


P1

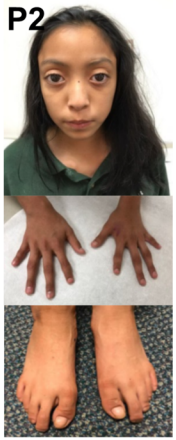
P2


P3

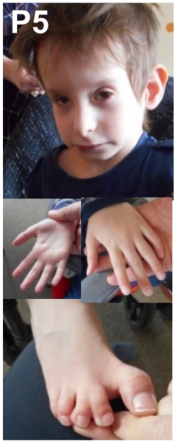
P5


P9

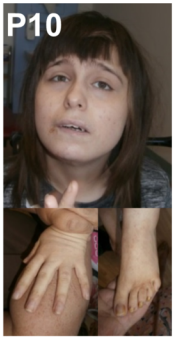
P10


P11

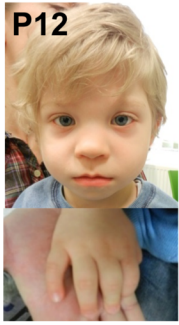
P12


P13


P14

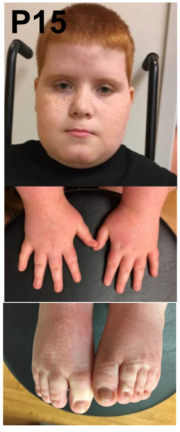
P15

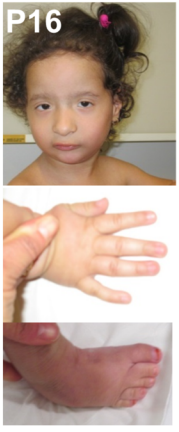
P16

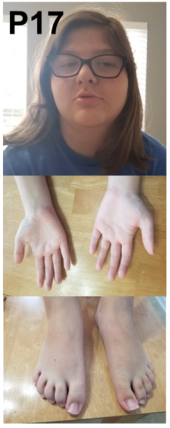
P17


P18


P19

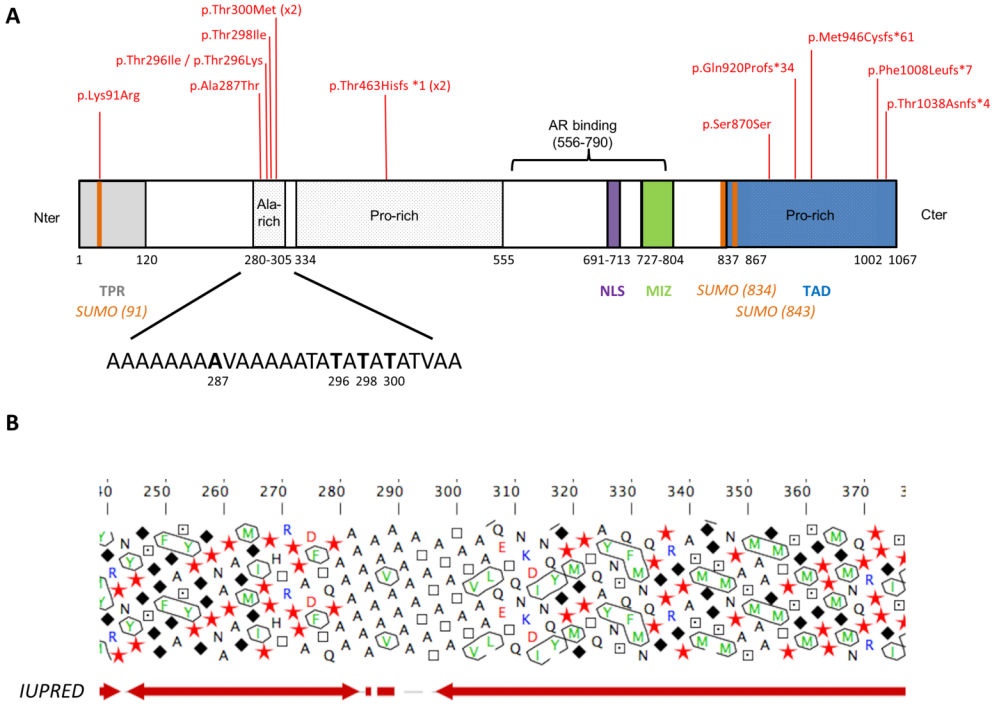
A
p.Thr300Met (x2)
p.Thr298Ile
p.Thr296Ile / p.Thr296Lys
p.Ala287Thr
p.Lys91Arg
p.Thr463Hisfs *1 (x2)
AR binding
(556-790)
p.Gln920Profs*34
p.Met946Cysfs*61
p.Phe1008Leufs*7
p.Ser870Ser
p.Thr1038Asnfs*4
Nter
Ala-
rich
Pro-rich
Pro-rich
Cter
1
120
280-305
334
555
691-713
727-804
837
867
1002
1067
TPR
SUMO (91)
NLS
MIZ
SUMO (834)
SUMO (843)
TAD
AAAAAAAAVAAAAATATATATATVAA
287
296
298
300
B
250
260
270
280
290
300
310
320
330
340
350
360
370
IUPRED

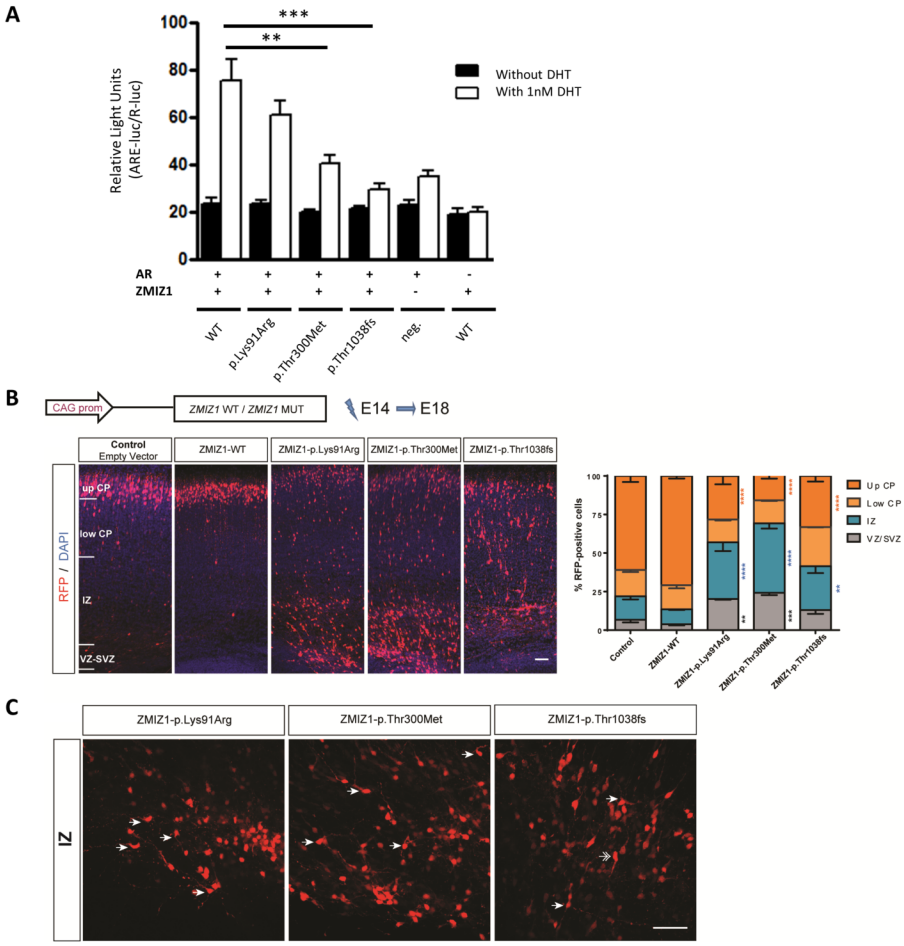
A
Relative Light Units
(ARE-luc/R-luc)
100
80
60
40
20
0
***
**
Without DHT
With 1nM DHT
AR
ZMIZ1
WT
p.Lys91Arg
p.Thr300Met
p.Thr1038fs
neg.
WT
B
CAG prom
ZMIZ1 WT / ZMIZ1 MUT
E14
E18
Control
Empty Vector
ZMIZ1-WT
ZMIZ1-p.Lys91Arg
ZMIZ1-p.Thr300Met
ZMIZ1-p.Thr1038fs
up CP
low CP
IZ
VZ-SVZ
RFP / DAPI
% RFP-positive cells
Up CP
Low CP
IZ
VZ/SVZ
C
ZMIZ1-p.Lys91Arg
ZMIZ1-p.Thr300Met
ZMIZ1-p.Thr1038fs
IZ